EPR observation of pseudostatic and dynamic Jahn-Teller effects in Cu^{2+}-doped $MgNa_2(SO_4)_2\cdot 4H_2O$ and $CoNa_2(SO_4)_2\cdot 4H_2O$ single crystals

Sushil K. Misra and Jiansheng Sun*
Physics Department, Concordia University, 1455 de Maisonneuve Boulevard West, Montreal, Quebec, Canada H3G 1M8
(Received 18 January 1991)

X-band EPR studies on single crystals of Cu^{2+}-doped $MgNa_2(SO_4)_2\cdot 4H_2O$ and $CoNa_2(SO_4)_2\cdot 4H_2O$ have been made over the temperature range 113–398 K. Two physically equivalent but magnetically inequivalent Cu^{2+} complexes have been observed in each sample. The Cu^{2+} spin-Hamiltonian parameters were estimated in these crystals and found to be independent of temperature below the respective transition temperatures from pseudostatic to dynamic Jahn-Teller states, and dependent on temperature above the transition temperatures, which are 339±2 K and 347±2 K for $MgNa_2(SO_4)_2\cdot 4H_2O$ and $CoNa_2(SO_4)_2\cdot 4H_2O$, respectively. In addition, the spin-lattice relaxation times (τ) of the paramagnetic host ions Co^{2+} in $CoNa_2(SO_4)_2\cdot 4H_2O$ lattice have been estimated at various temperatures, using the Cu^{2+} EPR linewidths and an expression appropriate to crystals consisting of two different kinds of paramagnetic ions. The temperature variation of τ with temperature suggests the predominance of Kramer's Raman process of spin-lattice relaxation over the range 280–300 K.

I. INTRODUCTION

The EPR technique has been extensively employed to study the Jahn-Teller effect (JTE).[1–4] Many observations of the JTE have been reported on Cu^{2+}-doped single crystals which have high-symmetry host sites. When the kinetic energy of the ligand ions can be neglected, a static JTE is observed, otherwise a dynamic JTE manifests itself. The present EPR studies of Cu^{2+}-doped $MgNa_2(SO_4)_2\cdot 4H_2O$ (hereafter MNST) and $CoNa_2(SO_4)_2\cdot 4H_2O$ (hereafter CNST) crystals are made in the 113–398-K temperature range; this makes it possible to observe both the pseudostatic JTE and the dynamic JTE, in the diamagnetic MNST and paramagnetic CNST host lattices.

MNST and CNST crystals belong to a family of hydrated double sulfates other than Tutton salts, known as astrakanites.[5] Unlike Tutton salts, for which extensive EPR studies have been reported, EPR studies on only CNST and $ZnNa_2(SO_4)_2\cdot 4H_2O$ (ZNST) crystals in the family of astrakanites have been reported.[6–11] No EPR study on MNST has, so far, been reported. For CNST, Jain and Yadav[12] estimated spin-lattice relaxation time (τ) of the host-ion Co^{2+}, from the EPR linewidth of an impurity ion Mn^{2+}, using we believe an incorrect formula. Emphasis in this paper is on the determination of the ground state of Cu^{2+} ion in these host lattices, observation of the pseudostatic and dynamic Jahn-Teller effects, and estimation of τ for host ions, Co^{2+}, in CNST from the impurity Cu^{2+} EPR linewidths using the correct formula.[13]

II. SAMPLE PREPARATION AND CRYSTAL STRUCTURE

Single crystals of MNST and CNST, doped with Cu^{2+}, were grown at room temperature (RT) by slow evaporation from saturated aqueous solutions, containing stoichiometric amounts of $MgSO_4\cdot 7H_2O$ and $CoSO_4\cdot 7H_2O$, respectively, and Na_2SO_4, to which a small quantity of $CuSO_4\cdot 5H_2O$ powder was added, so that there was one Cu^{2+} ion for every 100 M^{2+} (M=Mg, Co) ions. Crystals, suitable for EPR measurements, about $3\times 2\times 2$ mm^3 in size, grew in about 4 weeks. The growth habits of MNST and CNST single crystals are exhibited in Fig. 1.

MNST and CNST crystals are isostructural to that of ZNST, which is monoclinic with space group $P2_1/a$, containing two formula units per unit cell.[5] The unit-cell parameters for MNST are $a=1.104$ nm, $b=0.815$ nm, $c=0.549$ nm, $\beta=100.66°$,[5] being similar to ZNST. For CNST, the unit-cell parameters have not been reported but Vegard's law[14] may be used to estimate their values: $a=1.159$ nm, $b=0.855$ nm, $c=0.576$ nm, and $\beta=100.7°$. As seen from Fig. 2, which exhibits the structure of MNST and CNST, an M^{2+} ion is surrounded by four oxygen atoms lying approximately in a plane, of which two, referred to as $H_2O(1)$, belong to two different

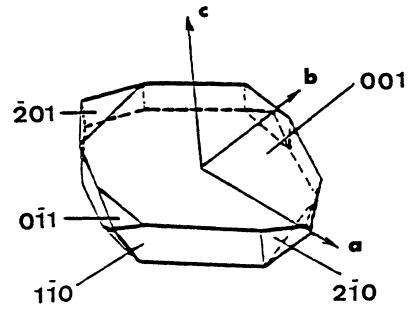

FIG. 1. The growth habit of MNST and CNST crystals (Ref. 8).

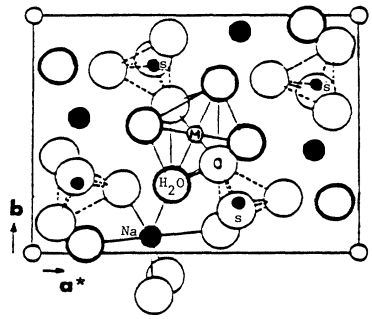

FIG. 2. The structure of MNST and CNST crystals as projected onto the a^*b plane ($a^*=a\sin\beta$) (Ref. 7).

water molecules, and the other two, referred to as O(3), belong to the two sulfate groups. The M^{2+}-O^{2-} distance in the oxygen plane is about 0.202 nm. Perpendicular to this plane, the oxygen atoms of the two water molecules, referred to as $H_2O(2)$, are coordinated to the M^{2+} ion at a distance of about 0.224 nm. The $MO_2(H_2O)_4$ complex forms an elongated tetragonally distorted octahedron, corresponds approximately to the point group C_{4v}. The positions of the two M^{2+} ions in the unit cell are at (0, 0, 0) and (1/2, 1/2, 0).

III. EXPERIMENTAL ARRANGEMENT AND EPR DATA

The EPR spectra were recorded on a Varian X-band V4506 spectrometer. The crystal was placed inside a TE_{102} Varian cavity. Diphenyl picryl hydrazyl (DPPH), for which $g=2.0036\pm0.0002$, was used as a reference to check the accuracy of the resonant frequency and the magnetic-field values. The line positions were determined with an accuracy of 0.05 mT. The temperature stability was better than 0.5 K.

For both the Cu^{2+}-doped MNST and CNST crystals, the angular variations of EPR line positions were recorded for the orientation of the external magnetic field (**B**) in three mutually perpendicular planes at every 5° interval. The largest flat plane (Fig. 1), which contains the crystallographic a and b axes, was chosen to define the XY plane with **Y**‖**b**; thus the z axis is parallel to the crystallographic c axis.

A. Room-temperature EPR spectra

For both Cu^{2+}-doped MNST and CNST crystals, RT EPR spectra indicated that there were present two physically equivalent, but magnetically inequivalent Cu^{2+} complexes in the unit cell of MNST and CNST, referred to as Cu^{2+} ions I and II. These arise from the two magnetically inequivalent M^{2+} sites, i.e., they can be distinguished by a magnetic field, in the unit cell of MNST or CNST, substituted for by the Cu^{2+} ions; the two sites have physically equivalent environments, being related to each other by an appropriate transformation. For the orientation of the Zeeman field (**B**) in the ZY and XY planes, there were observed two sets of four allowed Cu^{2+} hyperfine (hf) lines ($\Delta M=\pm1$, $\Delta m=0$, where M and m are, respectively, the electronic and magnetic quantum numbers for Cu^{2+} with electron spin $S=1/2$, and nuclear spin $I=3/2$ for each ^{63}Cu and ^{65}Cu isotope) with equal intensities. The hf lines due to the two isotopes of copper, ^{63}Cu (69.09% abundance) and ^{65}Cu (30.91% abundance), were not resolved. The two sets of hf lines were coincident for **B** along the **Y** (**b**) axis. For **B** in the ZX (a^*c plane; $a^*=a\sin\beta$), there was observed only one set of four Cu^{2+} hf lines, implying that the two sets of hf lines due to the two Cu^{2+} complexes in the unit cell are coincident for **B** in this plane. This is only possible if the ZX (a^*c) plane is a plane of symmetry for the two magnetically inequivalent Cu^{2+} ions in the unit cell. Thus, the EPR spectra of the two Cu^{2+} ions, which substitute for the two M^{2+} ions in the unit cell of MNST and CNST (Sec. V), are consistent with the crystallographic symmetry.[5]

At RT, the Cu^{2+} EPR linewidths (ΔB) in MNST and CNST were 4.0 mT (Fig. 3) and 8.5 mT, respectively. This is similar to other Cu^{2+}-doped hosts, in which the spin-lattice relaxation (SLR) processes of Cu^{2+} are enhanced by the tunneling effect between different spin states of Cu^{2+} in the Jahn-Teller systems,[1,2,4] resulting in shorter SLR times. Because of large ΔB, the two sets of hf lines from the two isotopes, ^{63}Cu and ^{65}Cu were not resolved. For **B** in the ZX and ZY planes in CNST, even the four hf lines were not clearly resolved, being broadened by interaction of the Cu^{2+} ion with the paramagnetic host Co^{2+} ions.

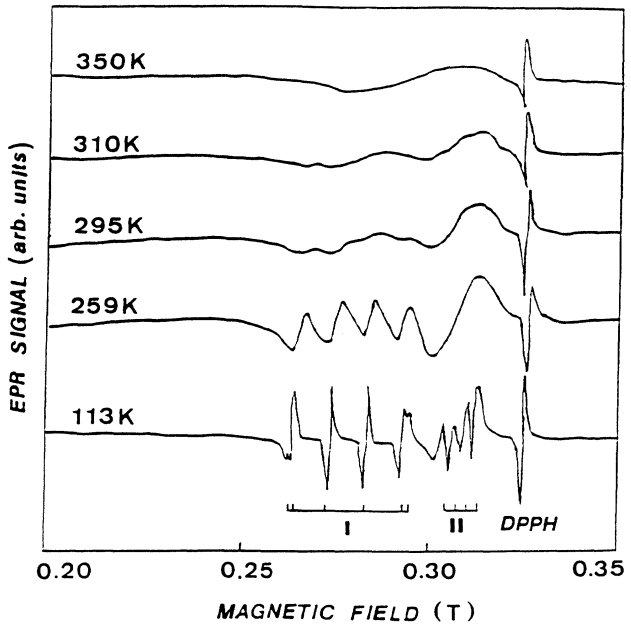

FIG. 3. Temperature variation of the Cu^{2+} EPR spectra in MNST single crystal, for **B** in the XY plane, 35° away from the Y axis. The Cu^{2+} hyperfine lines due to the two isotopes (^{63}Cu and ^{65}Cu) are clearly resolved at 113 K. For $T>T_{JT}(=347\text{ K})$, the two sets, corresponding to two magnetically inequivalent ions I and II, of four hf lines merge to form a single broad and isotropic line, corresponding to $g=2.20$ The splitting of the two outer lines of Cu^{2+} ion I is due to the two isotopes of copper, the lines belonging to ^{65}Cu are lying at the extremes.

B. EPR spectra below room temperature

EPR line positions of Cu^{2+} in MNST and CNST did not change significantly with temperature, implying a temperature independence of their spin-Hamiltonian parameters (Sec. IV). However, linewidths (ΔB) did exhibit a large change, as seen from Fig. 3. For MNST, the linewidth decreased at lower temperatures, to 1.2 mT at 113 K. The hf lines of the two different isotopes became clearly resolved at 113 K. The narrower linewidth is due to longer SLR time of the impurity ion Cu^{2+} (τ_{Cu}) at lower temperatures.

τ_{Cu} can be estimated from the expression $\tau_{Cu}=\hbar/(g\mu_B\Delta B)$,[1,15] neglecting the spin-spin interaction between Cu^{2+}-Cu^{2+} pairs. (Here g is the spectroscopic splitting factor.) The value of τ_{Cu} in MNST was estimated to be 6.9×10^{-9} sec at RT, and 2.7×10^{-8} sec at 113 K.

The Cu^{2+} EPR linewidth in CNST increased significantly, as the temperature was decreased from RT due to paramagnetic interactions with the host ions. Below 280 K, the hf lines were no longer resolved. This is due to an increase of τ of host ions Co^{2+} (Sec. VI).

C. EPR spectra above room temperature

Above RT, the linewidths of Cu^{2+} in both MNST and CNST hosts increased with temperature. Above $T_{JT}=347\pm2$ K in MNST and 339 ± 2 K in CNST, only one broad line was observed, as exhibited in Fig. 3. The line became isotropic, i.e., both the position of the line and its width were independent of the orientation of **B**. For $T>T_{JT}$, the two sets of Cu^{2+} hf lines, which were found to be magnetically inequivalent at room and lower temperatures, became coincident to form only one broad line. That is, the two sets of Cu^{2+} EPR spectra became magnetically, as well as physically, equivalent. No further change in the linewidth was observed as the temperature was raised to 398 K, above which both MNST and CNST crystals were destroyed due to heat. The single isotropic line for each of the MNST and CNST hosts for $T>T_{JT}$ corresponds to $g=2.20$ for Cu^{2+}, which is the average of the three principal values of the g matrix at temperatures below T_{JT} in each case. (See Sec. IV.) The behavior of EPR spectra above T_{JT} can be well explained to be due to dynamic JTE. (See Sec. VII.)

IV. SPIN-HAMILTONIAN PARAMETERS

The EPR line positions of Cu^{2+}, for any ^{63}Cu or ^{65}Cu isotope, in MNST and CNST hosts were fitted to the following spin-Hamiltonian:[1]

$$\mathcal{H}=\mu_B\mathbf{B}\cdot\mathbf{g}\cdot\mathbf{S}+\mathbf{S}\cdot\mathbf{A}\cdot\mathbf{I}\ , \tag{1}$$

where μ_B is the Bohr magneton, $S(=1/2)$ is the electronic spin, and $I(=3/2)$ is the nuclear spin of Cu^{2+} for each of the ^{63}Cu and ^{65}cu nuclear isotopes. The nuclear quadrupolar interaction has not been included in Eq. (1), since it has negligible effect on the allowed EPR line positions.

The principal values of the g^2 and A^2 tensors and their direction cosines were evaluated from the EPR line positions, for one of the two magnetically inequivalent Cu^{2+} ions I and II, by the use of a least-squares fitting procedure,[16,17] utilizing numerical diagonalization of the spin-Hamiltonian matrix on a digital computer. The principal values and direction cosines of the g and A matrices so evaluated for MNST (at RT) and CNST (at 113 K), for Cu^{2+} ion I, which were found to be the same as those for Cu^{2+} ion II, are listed in Tables I and II, respectively. For both MNST and CNST, the values of the spin-Hamiltonian parameters at room and lower temper-

TABLE I. Principal values and direction cosines of the g and A matrices of Cu^{2+} ion I in MNST single crystal at 113 K. The principal values of g and A matrices for Cu^{2+} ion II were found to be the same as those for ion I. All the values at room temperature were found to be the same as those listed here within experimental errors. Thus the principal values of the A matrix at RT are the averages of those for ^{63}Cu and ^{65}Cu isotopes because the corresponding lines were not resolved. The principal values of g are dimensionless, while those of A are expressed in GHZ. The indicated errors are those estimated by the use of a statistical method (Ref. 23). The direction cosines of the g^2 tensor (X', Y', Z') are given with respect to the X, Y, and Z axes, while those of the A^2 tensor (X'', Y'', Z'') are expressed relative to (X', Y', Z').

Isotope	Principal Value	Direction cosine Z/Z'	X/X'	Y/Y'
	$g_{z'}=2.3991\pm0.0030$	0.0510	0.2027	0.9779
	$g_{x'}=2.1979\pm0.0030$	0.7258	0.6651	−0.1758
	$g_{y'}=2.0299\pm0.0030$	−0.6860	0.7187	−0.1132
^{65}Cu	$A_{z''}=0.4430\pm0.0060$	0.9760	−0.0020	0.2176
	$A_{x''}=0.2513\pm0.0060$	0.0097	0.9994	−0.0034
	$A_{y''}=0.2060\pm0.0060$	−0.2174	0.0355	0.9755
^{63}Cu	$A_{z''}=0.4202\pm0.0060$	0.9999	0.0017	−0.0024
	$A_{x''}=0.2427\pm0.0060$	−0.0018	0.9988	−0.0499
	$A_{y''}=0.1986\pm0.0060$	0.0023	0.0499	0.9988

TABLE II. Principal values and direction cosines of the g and A matrices of Cu^{2+}-doped CNST single crystal at room temperature. Here, the principal values of the A matrix represent the averages of those for the ^{63}Cu and ^{65}Cu isotopes, since the hf lines due to the two isotopes were not resolved due to larger Cu^{2+} EPR linewidths observed in this paramagnetic host. For more details see the caption of Table I.

Principal value	Direction cosine		
	Z/Z'	X/X'	Y/Y'
$g_{z'}=2.4023\pm0.0030$	0.0110	0.4282	0.9036
$g_{x'}=2.1926\pm0.0030$	−0.3588	0.8452	−0.3961
$g_{y'}=2.0256\pm0.0030$	−0.9334	−0.3198	0.1629
$A_{z''}=0.3678\pm0.0060$	0.9999	−0.0146	0.0060
$A_{x''}=0.2363\pm0.0060$	−0.0153	−0.9923	0.1233
$A_{y''}=0.1679\pm0.0060$	−0.0041	0.1234	0.9924

atures were found to be the same, within experimental error, except that, at RT, the principal values of the A matrix should be taken to be the average of those for ^{63}Cu and ^{65}Cu isotopes as determined at 113 K, because the corresponding lines were not resolved at RT.

It is seen from Tables I and II that the principal axes of the g^2 and A^2 tensors are coincident with each other, within experimental error, for either CNST, or MNST. It is also noted from Tables I and II that, although there exists a small difference in the direction cosines of the g matrix for Cu^{2+} in CNST and MNST with respect to the respective unit-cell vectors, the principal values of the g and A matrices of Cu^{2+} in MNST and CNST are found to be quite close to each other. This is similar to the case of VO^{2+} in different Tutton salts,[18] and can be explained to be due to the fact that the host M^{2+} ions are not the nearest neighbors of the impurity ion Cu^{2+} (they are next-nearest neighbors); thus, they play rather insignificant roles in determining the values of the g, A matrices of Cu^{2+} in these hosts.

V. POSITION AND LOCAL SYMMETRY OF Cu^{2+} IONS

We assume that the site of an M^{2+} ion, which lies at the center of a $MO_2(H_2O)_4$ complex, is the most probable site for substitution by a Cu^{2+} ion, forming a $CuO_2(H_2O)_4$ complex. The Cu^{2+} ions I and II substitute for two different M^{2+} sites in the unit cell. Sastry and Sastry[10] concluded, from their EPR study of Cu^{2+}-doped ZNST, that the orientation of the principal Z axis of the g matrix was along the Zn^{2+}-$H_2O(1)$ direction. However, the present direction cosines of the g matrices for MNST and CNST do not indicate any correlation between the orientations of the principal axes of g matrices and the bond directions in the $MO_2(H_2O)_4$ complex of the MNST and CNST crystals, similar to the case of Gd^{3+} in ZNST.[9]

When a Cu^{2+} ion substitutes for a M^{2+} ion, it introduces a local distortion of the original $MO_2(H_2O)_4$ complex due to the difference of its ionic radius from those of the host ions M^{2+}. In addition, the Cu^{2+} ion, being a Jahn-Teller ion, introduces a Jahn-Teller distortion (Sec. VII). Due to these two types of distortions, the three principal values of the g matrices of Cu^{2+}, in both MNST and CNST, become different from each other below the respective Jahn-Teller transition temperature (Tables I and II), indicating a lower, orthorhombically distorted octahedral, symmetry at the Cu^{2+} ion in the $CuO_2(H_2O)_4$ complex.

VI. HOST-ION SPIN-LATTICE RELAXATION TIME (τ) of Co^{2+} IN CNST

τ of the host paramagnetic ions Co^{2+} in CNST can be estimated, using the contribution to the EPR linewidth of the impurity ion Cu^{2+} by the paramagnetism of the host ions, $\Delta B'$, by the use of the following expression:[13]

$$\tau=(3\Delta B' g^2\mu_B)/(110hg'\langle\Delta\nu^2\rangle)\ , \tag{2}$$

where μ_B, h, g, and g' are, respectively, Bohr's magneton, Planck's constant, the impurity-ion Landé's factor, and the host-ion Landé's factor. $\Delta B'$ is obtained by subtracting, from the observed impurity-ion linewidth, the linewidth of the impurity ion is an isostructural diamagnetic host.[18] Misra and Orhun[13] showed that $\langle\Delta\nu^2\rangle$, the second moment for the impurity ion for crystals containing two different species of magnetic ions can be expressed, when the distances between the impurity Cu^{2+} ions are considered to be quite large as in the present case, as

$$\langle\Delta\nu^2\rangle=\tfrac{1}{3}S'(S'+1)h^{-2}\left[NJ_p^2+gg'\mu_B^4\mu_0^2\sum_{k'}^{N}(1-3\gamma_{jk'}^2)^2 r_{jk'}^{-6}+2J_p gg'\mu_B^2\mu_0\sum_{k'}^{N}(1-3\gamma_{jk'}^2)r_{jk'}^{-3}\right]\ . \tag{3}$$

In Eq. (3), N, S', J_p, μ_0, $r_{jk'}$, and $\gamma_{jk'}$ are the number of host-ion neighbors considered, the effective spin of the host ion, the average impurity-host pair-exchange constant, the permeability constant, the distance between j and k' ions, and the direction cosines of $r_{jk'}$ with the external Zeeman field, **B**, respectively. The primed quantities refer to the host ions while the unprimed ones to the impurity ions.

For the calculation of the second moment $\langle \Delta\nu^2 \rangle$ in Cu^{2+}-doped CNST, it was found sufficient to consider only up to the fifth-nearest neighbors, i.e., a total of 20 Co^{2+} ions ($N=20$). In the estimation of τ, the g' value for Co^{2+} ($=3.866$) was chosen to be the average of the three principal values of the g matrix (g'_1, g'_2, g'_3) of Co^{2+} in ZNST host; these have been reported previously.[8] The value of the exchange constant J_p for the Cu^{2+}-Co^{2+} pairs has not been determined experimentally. However, it was found that the variation of J_p in the range of 0.0–3.0 GHz did not affect the value of τ significantly, indicating that for CNST only the dipolar interaction is of importance in determining τ. Accordingly, the value of J_p was chosen to be 0.3 GHz for the present estimates. The value of $\Delta B'$ at any temperature in the 280–330-K temperature range was estimated by subtracting from the total Cu^{2+} EPR linewidth in the paramagnetic CNST host the Cu^{2+} linewidth in the diamagnetic MNST host. It was not possible to measure the Cu^{2+} linewidth beyond the temperature range 280–330 K because of the broadening experienced by the EPR lines.

Finally, the value of τ of host-ions Co^{2+} in CNST was estimated to be 3.10×10^{-14} sec at RT. For comparison, Jain and Yadav[12] reported that τ of Co^{2+} in CNST was 1.66×10^{-12} sec using a different formula, a value 2 orders of magnitude larger than the presently estimated value. Further, the present values of τ can be fitted to the temperature (T), within experimental error, to $\tau^{-1}=AT^9$, where $A=5.64\times10^8$ $\text{sec}^{-1}\text{K}^{-9}$, in the 280–330-K temperature range. This temperature behavior of τ is consistent with that expected when the Kramer's Raman process of SLR is predominant.[1,19]

VII. JAHN-TELLER EFFECT

A. Ground state of Cu^{2+}

When the six ligands of a Cu^{2+} ion, in an octahedral sixfold coordination, form a regular octahedron, the ground state of the Cu^{2+} ion is the twofold degenerate E_g state. The degeneracy of the ground state of the Cu^{2+} ion is usually removed by a Jahn-Teller distortion.[1,2] The M^{2+} sites originally have an elongated tetragonally distorted octahedral coordination with the ligands, as revealed by x-ray data. However, due to the Jahn-Teller distortion the principal values of the g matrices of Cu^{2+} in MNST and CNST exhibit a lower, namely, orthorhombically distorted octahedral, symmetry at RT and lower temperatures. According to crystal-field theory, the orbital doublet E_g of the Cu^{2+} ion is split in a field of orthorhombic symmetry, the lower state being either $|X^2-Y^2\rangle$ or $|3Z^2-r^2\rangle$; which one of these two is predominant can be determined from the value of the parameter R,[2] which is defined as $R\equiv(g_x-g_y)/(g_z-g_x)$, where $g_z>g_x>g_y$, are the principal values of the g matrix of Cu^{2+} in the host lattice. When the R value is greater than unity, a predominantly $|3Z^2-r^2\rangle$ ground state is expected, while a predominantly $|X^2-Y^2\rangle$ ground state is expected when it is less than unity. Since, in the present case, the calculated R value is less than unity at RT and below, the predominant ground state of Cu^{2+} ion in both the MNST and CNST hosts, is $|X^2-Y^2\rangle$ with an admixture of the excited state $|3Z^2-r^2\rangle$.

B. Pseudo-Jahn-Teller effect

If the splitting between the ground state $|X^2-Y^2\rangle$ and the excited state $|3Z^2-r^2\rangle$, of Cu^{2+} is sufficiently small, a mixing of the two states by coupling with the lattice vibrations becomes quite possible. The vibronic mixing of the close-lying (pseudo degenerate) levels $|X^2-Y^2\rangle$ and $|3Z^2-r^2\rangle$ due to the interaction of the Cu^{2+} ion with its ligands manifests itself as a pseudostatic JTE.[2,20]

The molecular and electronic structures of the Cu^{2+} ion, surrounded by six ligands of octahedral or trigonal distortion, is conventionally described in terms of Jahn-Teller coupling between the doubly degenerate electronic (E_g) and vibrational (ε_g) states of the octahedral complex.[20] Assuming a harmonic-vibrational potential, and taking into consideration only the linear coupling terms, leads to the well-known Mexican-hat potential surface. The geometry of the Cu^{2+} complex fluctuates between the various conformations of D_{4h} and D_{2h} symmetries, which are generated by linear combinations of Q_θ and Q_ε, the components of the ε_g vibrational mode. Q_θ and Q_ε are conventionally expressed as $Q_\theta=\rho\cos\phi$ and $Q_\varepsilon=\rho\sin\phi$ in terms of a polar coordinate system (ρ,ϕ). When higher-order coupling terms are included, the perimeter of the Mexican hat becomes warped giving rise to three equivalent minima whose projections correspond to different ϕ values in the (Q_θ,Q_ε) space. Finally, the Mexican-hat potential results in three equivalent potential valleys. However, as pointed out by Ham,[4] a strain, having a tetragonal component, that may be present, as indicated by the three different principal values of the g matrices of Cu^{2+} in MNST and CNST, destroys the equivalence of the three potential valleys. When only the lowest potential valley is occupied at low temperatures, i.e., when $\Delta E > k_B T$ (ΔE is the energy difference between the lowest potential valley and the next-lying potential valleys), the principal values of the g matrix of Cu^{2+} are not expected to be very temperature dependent, in accordance with the present observations. Further, in the present case, only one set of hf lines for each of the two magnetically inequivalent Cu^{2+} sites was observed, implying that only the lowest potential valley is occupied. For, otherwise, as seen in the case of Cu^{2+}-doped $Zn(C_4H_4N_2)SO_4\cdot3H_2O$ single crystal,[21] three physically equivalent sets of hf lines should be observed for each

magnetically inequivalent Cu^{2+} site.

The above interpretation of the EPR spectra of Cu^{2+}-doped MNST and CNST at room and lower temperatures, in terms of pseudo-JTE, wherein the lowest-lying levels of the E state lie extremely close to each other but are not degenerate, is equivalent to that of the "static" JTE, wherein the lowest levels of the E state are degenerate, the degeneracy being lifted by a Jahn-Teller distortion, as described by Abragam and Bleaney.[1] This is consistent with the treatment of an E-state ion in a tetragonal crystal field, by Bir,[22] for a tetragonally distorted octahedral Cu^{2+} complex, such as $[Cu(H_2O)_6]^{2+}$.

C. Dynamic Jahn-Teller effect

Above RT, the hf lines of Cu^{2+} in both MNST and CNST became much broader because of decreased Cu^{2+} SLR times (Sec. III). A single isotropic Cu^{2+} line in MNST and CNST hosts was observed for $T > T_{JT}$, where $T_{JT} = 347$ and 339 K, respectively. This is characteristic of type I dynamic JTE.[4] This occurs when the rate of tunneling though the barrier, at higher temperatures, from one distorted configuration, or Jahn-Teller potential valley, of the complex to another exceeds the frequency difference between the corresponding EPR resonance lines for the different distorted configurations.[4] When dynamic JTE occurs $g_z = g_x = g_y = g_e - 4\lambda/\Delta$, which is equal to the average of the three principal values of the g matrix at $T < T_{JT}$, for both the Cu^{2+} ions I and II in the unit cell.[21] Here, $g_e (= 2.0023)$ is the g value of the free electron, λ is the spin-orbit coupling constant for the free Cu^{2+} ion ($= -830$ cm^{-1}), and Δ is the octahedral crystal-field constant for Cu^{2+} ion. For the typical value of $\lambda/\Delta = -0.05$ for Cu^{2+} ion,[1] the value of $(g_e - \lambda/\Delta)$ is 2.20, being the same as the presently observed g values at $T \geq T_{JT}$ for both the Cu^{2+} ions I and II in MNST and CNST and the average of the three principal values of g at $T < T_{JT}$.

Since the EPR line position and linewidth for Cu^{2+} in each of MNST and CNST were independent of the orientation of **B** at higher temperatures ($T > T_{JT}$), the "oriented" and "random" strains should be very small compared to $k_B T$. This is because the center of the EPR line depends on the orientation of **B** if the "oriented" strains are large, while the EPR linewidth depends on the orientation of **B** if the "random" strains are large.[4]

VIII. CONCLUDING REMARKS

(i) The main features of Cu^{2+} EPR spectra in diamagnetic MNST and paramagnetic CNST crystals are the same, except for a difference in the EPR linewidth, its temperature dependence, and T_{JT}. Both samples were interpreted as exhibiting a pseudostatic JTE at $T < T_{JT}$, and a dynamic JTE at $T > T_{JT}$. This implies that the host paramagnetic ions do not have any significant effect as compared to that due to the diamagnetic host ions. The reason as to why not many studies have been made on JTE in Cu^{2+}-doped paramagnetic hosts is that paramagnetic hosts are characterized by a larger EPR linewidth and consequently yield poorer resolution of EPR spectra.

(ii) Two magnetically inequivalent, but physically equivalent Cu^{2+} complexes have been observed in both MNST and CNST hosts below T_{JT}. The Cu^{2+} ion enters the site of a M^{2+} (M=Mg, Co) ion, forming a $CuO_2(H_2O)_4$ complex, which has an orthorhombically distorted octahedral symmetry, as indicated by the three different principal values of the g matrices at $T < T_{JT}$.

(iii) Below T_{JT}, a pseudo-JTE was observed for both the samples. At these temperatures, Cu^{2+} occupies only the lowest Jahn-Teller potential valley. However, at temperatures above T_{JT}, a dynamic JTE was observed, wherein Cu^{2+} ions occupy the three Jahn-Teller valleys with almost equal probabilities. The transition between the two kinds of JTE was found to take place at $T_{JT} = 347 \pm 2$ K and 339 ± 2 K for MNST and CNST, respectively.

(iv) The temperature dependences of Cu^{2+} EPR linewidths for MNST and CNST have been explained to be due mainly to the SLR of the impurity-ion Cu^{2+} in the diamagnetic MNST host, and that of the host-ion Co^{2+} in the paramagnetic CNST host. The SLR times (τ) of the impurity ion Cu^{2+} in MNST and that of the host ions Co^{2+} in CNST, have been estimated. From the temperature variation of τ the predominant spin-lattice relaxation process of host-ion Co^{2+} in CNST, in the 280–330-K temperature range, has been deduced to be the Kramer's Raman process.

ACKNOWLEDGMENT

The authors are grateful to the Natural Sciences and Engineering Research Council of Canada for partial financial support (Grant No. OGP0004485).

*On leave of absence from Center of Materials Analysis, Nanjing University, Nanjing, Jiangsu 210008, the People's Republic of China.

[1] A. Abragam and B. Bleaney, *Electron Paramagnetic Resonance of Transition Ions* (Clarendon, Oxford, 1970).

[2] S. K. Misra and C. Wang, Magn. Reson. Rev. **14**, 157 (1990).

[3] H. Bill, in *Dynamical Jahn-Teller Effect in Localized Systems*, edited by Yu. E. Rerlin and M. Wager (Elsevier, New York, 1984).

[4] F. S. Ham, in *Electron Paramagnetic Resonance*, edited by Geschwind (Plenum, New York, 1972).

[5] Von. M. Giglio, Acta Crystallogr. **11**, 789 (1958).

[6] V. K. Jain and P. Venkateswarlu, J. Phys. C **12**, 865 (1979).

[7] V. K. Jain, J. Phys. C **12**, 1403 (1979).

[8] G. R. Bulka, S. V. Vedenin, V. M. Vinokurov, T. A. Zakharchenko, N. M. Nizamutdinov, and R. S. Tukhvatullin, Kristallografiya **16**, 138 (1971) [Sov. Phys. Crystallogr. **16**, 107 (1971)].

[9] J. M. Gaite, G. R. Bulka, N. M. Hasanova, N. M. Nizamutdinov, and V. M. Vinofurov, J. Phys. C **19**, 2077 (1986).

[10] B. A. Sastry and G. S. Sastry, J. Phys. C **4**, L347 (1971).

[11] B. A. Sastry, B. Madhu, and K. M. Kar, Indian J. Phys. A **62**,

463 (1988).
[12]V. K. Jain and V. S. Yadav, Solid State Commun. **69**, 407 (1989).
[13]S. K. Misra and U. Orhun, Phys. Rev. B **39**, 2856 (1989).
[14]L. Vegard, Z. Kristallogr. **67**, 239 (1928).
[15]D. P. Breen, D. C. Krupka, and F. I. B. Williams, Phys. Rev. **179**, 241 (1969).
[16]S. K. Misra, Physica B **121**, 193 (1983).
[17]S. K. Misra, Physica B **124**, 53 (1984).
[18]S. K. Misra, J. Sun, and X. Li, Physica B **168**, 170 (1991).
[19]K. N. Shrivastava, Phys. Status. Solid B **117**, 437 (1983).
[20]B. Bersukev and V. Z. Polinger, in *The Dynamical Jahn-Teller Effect in Localized Systems* (North-Holland, Amsterdam, 1984).
[21]S. K. Misra and C. Wang, J. Phys. Condens. Matter **1**, 771 (1989).
[22]G. L. Bir, Fiz. Tver. Tela (Leningrad) **18**, 946 (1976) [Sov. Phys. Solid State **18**, 542 (1976)].
[23]S. K. Misra and S. Subramanian, J. Phys. C **15**, 7199 (1982).